

# Microscopic Calculations of Solvent Effects on Absorption Spectra of Conjugated Molecules

V. Luzhkov<sup>†</sup> and A. Warshel\*

Contribution from the Department of Chemistry, University of Southern California, Los Angeles, California 90089-1062. Received October 26, 1990

**Abstract:** Microscopic approaches for calculating absorption spectra of molecules in solutions are developed and examined. These methods evaluate self-consistently the relationship between the solute and solvent polarization, incorporating the potential from the permanent and induced solvent dipoles in the solute Hamiltonian. Two microscopic solvent models are examined in the framework of the present formulation. The first one is the simplified Langevin dipoles (LD) solvent model, which provides fast and reliable estimates of solvent effects on absorption spectra. The second involves an all-atom solvent model and molecular dynamics simulations of the fluctuations of the solvent and the solute. Use of the time dependent excitation energies of this model and the dispersed polaron formulation allows one to obtain the absorption line shapes of molecules in solutions. The relationship between the present treatments and earlier macroscopic treatments, which consider the spectrum as a function of an arbitrarily defined cavity radius, is discussed. It is pointed out that many of the conceptual problems associated with the macroscopic treatments become quite simple when one uses microscopic models. The performances of our approaches are examined by calculating solvent effects on the lowest  $\pi \rightarrow \pi^*$  transitions of various polyene aldehydes and merocyanine dyes. The agreement between the calculated and observed spectral shifts is encouraging, indicating that the present methods can provide useful tools for analyzing the spectra of chromophores in solutions and in biological sites.

## 1. Introduction

Theoretical studies of electronic spectra date back to the early days of quantum chemistry. Yet, despite this early start, most quantum mechanical studies have been confined to isolated molecules in the gas phase, while most experimental studies involve molecules in solutions. Thus, the development of methods capable of evaluating the spectra of molecules in solutions is one of the challenges of modern quantum chemistry.

In trying to account for the effect of the solvent on the spectrum of a given molecule, one has to evaluate the *change* in the solute-solvent interaction upon electronic excitation. This change may involve many factors such as dispersion, polarization, and Coulombic and charge transfer interactions. Yet the polarization and Coulombic interactions are expected to have the dominant effect, as long as we deal with electronic transitions that involve large changes in the solute charge distribution (provided the excited-state wave function is localized on the solute molecule rather than extended to the solvent region). This is, in fact, the assumption made by McRay and others<sup>2,3</sup> in their pioneering studies of solvent effects on absorption spectra. However, these early studies were formulated on a phenomenological level and involved macroscopic continuum models with an arbitrarily defined cavity radius as an adjustable parameter. Such treatments, which might seem quite reasonable in the first sight, lead to major problems when one tries to evaluate the absolute value of the solvent effect (rather than the trend associated with changes of solvent polarity). That is, the calculations are as reliable as their ability to reproduce the relevant solvation energies, and cavity treatments can give enormous errors when applied to cases that involve a large charge separation. This can be easily verified by the reader trying to reproduce the solvation energies of ion pairs (e.g., the examples of ref 4) using any cavity model. Furthermore, the macroscopic treatments present significant difficulties in consistent treatments of electronic excitations in polar solvents, where the induced dipoles of the solvent should adjust themselves to the charge distribution of the excited solute, while still responding to the polarization of the solvent permanent dipoles (which are kept at their ground state distribution). While macroscopic treatments of this problem are available (e.g., ref 3d) for cases where the solute's charge distribution can be represented by the dipole approximation, the treatment of more general charge distribution presents a major challenge. This challenge becomes

even more serious when the solvent polarization in the ground state involves saturation effects.

Microscopic studies of solvent effects on electronic spectra are quite limited, and with the exception of the preliminary studies of ref 4 we are not aware of microscopic studies that treated consistently the polarization of the solvent by the excited state of the solute (including the permanent and induced solvent polarization). Similarly, the progress in studies of environmental effects on the spectra of biological chromophores has been quite limited, despite the great interest in this problem. Apparently most attempts to estimate such effects have been based on the use of Coulomb's law with a low dielectric constant (e.g., refs 5 and 6) rather than on a consistent treatment of the solvation energies in the actual environment. A preliminary examination of a more consistent treatment was reported in a study of the spectral shift between the r and t states in hemoglobin.<sup>7</sup>

The proper quantum mechanical treatment of a solvated chromophore is far from being obvious. The main problem is associated with the fact that the multidimensional solute-solvent system involves an enormous number of degrees of freedom. Thus, one cannot expect to get meaningful results while treating the entire system by any rigorous quantum mechanical approach. Instead it is imperative to use an approximate treatment that separates the system into classical and quantum mechanical parts. Such a treatment should also be parametrized by using the relevant experimental properties (e.g., observed solvation energies) in order to get reliable results. Early attempts to treat microscopic solvent effects by quantum mechanical/classical separation were reported in refs 8 and 9. These studies used simplified dipolar solvent

(1) McRae, E. G. *J. Phys. Chem.* **1957**, *61*, 562.

(2) (a) Bayliss, N. S. *J. Chem. Phys.* **1950**, *18*, 292. (b) Lippert, E. *Acc. Chem. Res.* **1970**, *3*, 74. (c) Amos, A. T.; Burrows, B. L. *Adv. Quantum Chem.* **1973**, *7*, 289.

(3) (a) Kosower, E. M. *An Introduction to Physical Organic Chemistry*; John Wiley & Sons, Inc.: New York, 1968. (b) Mataga, N.; Kubota, T. *Molecular Interactions and Electronic Spectra*; Marcel Dekker, Inc.: New York, 1970. (c) Salem, L. *Electrons in Chemical Reactions: First Principles*; John Wiley & Sons, Inc.: New York, 1982. (d) Karelson, M.; Zerner, M. *C. J. Am. Chem. Soc.* **1990**, *112*, 9405.

(4) (a) Warshel, A. *J. Phys. Chem.* **1979**, *83*, 1640. (b) Warshel, A.; Russel, S. T. *Q. Rev. Biophys.* **1984**, *17*, 283.

(5) Honig, B.; Dinur, U.; Nakanishi, K.; Balogh-Nair, V.; Gawinowicz, M. A.; Arnaboldi, M.; Motto, M. G. *J. Am. Chem. Soc.* **1979**, *101*, 7084.

(6) Birge, R. R.; Hubbard, L. M. *J. Am. Chem. Soc.* **1980**, *102*, 2195.

(7) Warshel, A.; Lippicirella, A. *J. Am. Chem. Soc.* **1981**, *103*, 4664.

(8) Warshel, A.; Levitt, M. *J. Mol. Biol.* **1976**, *103*, 227.

<sup>†</sup>Permanent Address: Institute of Chemical Physics, Chernogolovka, Moscow Region, USSR.

models, which were incorporated consistently in the solute Hamiltonian, and took into account the solvent permanent and induced dipoles. A recent molecular dynamics (MD) study of the solvent effect on the absorption spectrum of formaldehyde<sup>10</sup> has demonstrated the feasibility of using more realistic solvent models with an extensive phase space exploration. However, this work has not considered the important effect of the solvent induced dipoles and the self-consistent effect of the change in the solute polarization (as a result of the solvent field) on the solvent polarization.

MD studies of electron transfer (ET) reactions in solutions<sup>11</sup> have demonstrated the feasibility of calculating absorption line shapes in solutions. That is, the evaluation of the dependence of rate constants on the corresponding reaction free energies is isomorphous to the evaluation of absorption line shapes. Thus, the dispersed polaron model,<sup>11</sup> developed for studies of quantum mechanical rate constants of ET reactions should provide a useful tool for studies of the vibronic line shape of electronic spectra in solutions. It is interesting to examine the practicality of such an approach in studies of the spectra of conjugated molecules in solutions.

This work describes and examines several strategies for calculating solvent effects on absorption spectra, following in part the philosophy and initial formulation of refs 4a and 8. Section 2 provides the theoretical background, considering the incorporation of the solvent permanent and induced dipoles in the solute Hamiltonian. The formulation developed is implemented with two solvent models: The first one is the simplified Langevin dipoles solvent model, and the other involves a more complete all-atom model and a MD simulation approach. Section 3 examines the performance of the present approaches in several well-defined test cases. It is demonstrated that these approaches can provide a powerful way for analyzing the spectra of molecules in solutions.

## 2. Theoretical Methods

**2.1. Spectral Shifts Due to Permanent Polarization.** To clarify our theoretical approach, we start by considering the rather simple case where the solvent molecules have a fixed charge distribution (neglecting electronic polarizability effects). This case can be treated by considering formally the solute-solvent system as a supermolecule and writing the molecular orbitals (MO) functions as a linear combination of the atomic orbitals (AO) of the entire system:

$$\phi_i = \sum_{\mu} v_{\mu i} \chi_{\mu}^s + \sum_{\lambda} v_{\lambda i} \chi_{\lambda}^s \quad (1)$$

where S and s designate the solute and solvent, respectively, the  $v$  are the MO coefficients, and the  $\chi$  are AO functions (which might involve more than one orbital per atom). We also assume that atomic orbitals  $\chi^s$  and  $\chi^s$  are orthogonal and use formally a CNDO-type all valence electron approximation. The coefficients  $v_{\mu i}^s$  and  $v_{\lambda i}^s$  can be obtained by solving the SCF equation for the supersystem.

$$\mathbf{F}v_i = \epsilon_i v_i \quad (2)$$

where the F matrix can be separated into blocks describing the solute-solute, solvent-solvent, and the solute-solvent interactions. The as-

$$\begin{bmatrix} \mathbf{F}^S & \mathbf{F}^{S_s} \\ \mathbf{F}^{S_s} & \mathbf{F}^s \end{bmatrix} \quad (3)$$

sumption that the solvent and solute AO are orthogonal to each other implies, within the CNDO approximation, that  $\mathbf{F}^{S_s} = 0$ ; the assumption that the overlap integral  $(\chi_{\mu}^s | \chi_{\lambda}^s) = 0$  implies, in this level of approximation, that  $\beta^{S_s} = 0$ , and therefore  $P_{S_s} = 0$  (where  $\beta$  and  $P$  designate, respectively, the relevant resonance integral and bond order). This also amounts to the neglect of charge transfer interaction between the solute and the solvent. Thus, we obtain two sets of solutions to the SCF

equation,  $\phi_i^s = (v_{\mu i}^s, 0)$  and  $\phi_j^s = (0, v_{\lambda j}^s)$ . This means that the coefficients  $v_{\lambda i}^s$  and  $v_{\mu j}^s$  are equal to 0, and that the MOs of the solute can be considered separately from the solvent MOs. Treating the complete F matrix within the CNDO-type approximation, we obtain for the solute part of the F matrix

$$F_{\mu\mu}^s = (F_{\mu\mu}^s)_0 - \sum_{B \in S} q_B \gamma_{AB} \quad \mu \in A \in S \quad (4)$$

$$F_{\mu\nu}^s = (F_{\mu\nu}^s)_0$$

$$q_B = \sum_{r \in B} (Z_r - P_{rr}) = Z_B - P_B$$

where the notation  $\mu \in A$  indicates that  $\mu$  may be any of the valence atomic orbitals on the Ath atom,  $(F_{\mu\mu}^s)_0$  designates the SCF matrix of the isolated solute molecule, A and B are, respectively, the solute and solvent atoms, and  $\gamma_{AB}$  is the electron-electron repulsion integral, which accounts here for the solvent influence on the solute electronic structure.  $q_B$ ,  $Z_B$ , and  $P_B$  are, respectively, the atomic charge, the core charge, and the atomic bond order for the Bth atom (see ref 7 for more details). In general, we can write eq 4 for any solvent charge configuration as<sup>8</sup>

$$F_{\mu\mu}^s = (F_{\mu\mu}^s)_0 - \sum_B e^2 q_B / r_{AB} = (F_{\mu\mu}^s)_0 - U_A \quad (5)$$

where  $\gamma_{AB}$  is approximated by  $e^2/r_{AB}$  and  $U_A$  designates the total potential from solvent atoms at the site of atom A. This equation applies to any solvent configuration, but as will be emphasized below we will have to consider those configurations that are at equilibrium with the solute charge distribution. Note that eq 5 is not a classical approximation but simply the result of fixing the solvent molecular orbitals and the corresponding charges (the  $q_B$ 's).

Using the dipole approximation for the solute-solvent interaction, we can express the diagonal elements of the solutes F matrix in the following form:

$$F_{\mu\mu}^s = (F_{\mu\mu}^s)_0 - \sum_k m_k r_{kA} / r_{kA}^3 \quad (6)$$

where  $m_k$  is the dipole of the kth solvent molecule and  $r_{kA} = r_A - r_k$ .

The excitation energies at a given solvent configuration can be obtained by solving the CI equation for the wave functions:

$$\Psi_i = \sum_n c_{in} \psi_n \quad (7)$$

where  $\psi_n$  represent a Slater determinant wave function, corresponding to the excitation from the SCF orbital  $n_1$  to  $n_2$ , and the coefficients vector  $c_i$  is obtained from the CI equation

$$\mathbf{A}c_i = E_{gf} c_i \quad (8)$$

where g and f denote ground and excited states, respectively, and  $E_{gf}$  is the excitation energy from the ground to the fth excited state. The elements of the CI matrix are given by

$$A_{nn} = \epsilon_{n_2} - \epsilon_{n_1} - (n_1 n_2 | n_1 n_2) + 2(n_1 n_2 | n_2 n_1) \quad (9)$$

$$A_{nm} = 2(m_1 n_2 | m_2 n_1) - (m_1 n_2 | n_1 m_2)$$

with

$$(ij|kl) = \int \int \phi_i(1)\phi_j(2)(1/r_{12})\phi_k(1)\phi_l(2) d\tau_1 d\tau_2 = \sum_{\mu\nu} v_{i\mu} v_{k\mu} v_{j\nu} v_{l\nu} \gamma_{\mu\nu} \quad (10)$$

Since the electronic excitation process is much faster than the reorientation time of the solvent dipoles, we can treat the present problem with the solvent permanent dipoles fixed at their ground-state configurations (the configurations obtained in response to the solute's ground-state charges). The evaluation of these solvent configurations depends, of course, on the model used and will be considered in section 2.3. It is important, however, to note that regardless of the actual solvent model used one must retain a self-consistent relationship between the solvent polarization and the corresponding ground-state charges of the solute,  $Q$ . This is done iteratively, starting with the gas-phase solute charges,  $Q^{(0)}$ , to obtain the solvent potential,  $U_s^{(0)}$ , which is then incorporated in eq 5 to give new solute charges,  $Q^{(1)}$  new solvent potential,  $U_s^{(1)}$ , and so on. Once we obtain a set of equilibrated solvent configurations (in the case of the LD model, we will have a single set that represents the average solvent polarization), we can use eq 5 to obtain the charge distribution of the solute in its ground and excited states and the spectral shift of  $E_{gf}$  in solution, which is evaluated as the difference between the solutions of CI equations for the solvated solute (sol) and the solute in the gas phase (gas), using

$$\Delta E_{gf}^{\text{perm}} = E_{gf}^{\text{sol}}(U_s^{\text{perm}}) - E_{gf}^{\text{gas}} \quad (11)$$

(9) Warshel, A. *Chem. Phys. Lett.* **1978**, *55*, 454.

(10) Blair, J. T.; Krogh-Jespersen, K.; Levy, R. M. *J. Am. Chem. Soc.*, in press.

(11) (a) Warshel, A.; Hwang, J.-K. *J. Chem. Phys.* **1968**, *84*, 4938. (b) Warshel, A.; Chu, Z. T.; Parson, W. W. *Science* **1989**, *246*, 112.

(12) (a) Beveridge, D. L.; DiCappia, F. M. *Annu. Rev. Biophys. Biophys. Chem.* **1980**, *18*, 43. (b) Warshel, A.; Aqvist, J. *Annu. Rev. Biophys. Biophys. Chem.* **1991**, in press.

(13) (a) *CRC Handbook of Chemistry and Physics*; Weast, R. C., Ed.; The Chemical Rubber Co.: Cleveland, OH, 1989. (b) Davies, M. *Some Electrical and Optical Aspects of Molecular Behavior*; Pergamon Press: London, 1965.

where  $U_{\mu}^{\text{perm}}$  is the vector whose components are the values of the solvent potential at the solute atoms (the  $U_{\mu\text{A}}^{\text{perm}}$  values) and the superscript "perm" indicates that we are only dealing with the permanent dipoles. The functional dependence of  $E_{\mu}^{\text{sol}}$  on  $U_{\mu}^{\text{perm}}$  indicates that the corresponding excitation energy is evaluated by adding  $U_{\mu}^{\text{perm}}$  to the SCF Hamiltonian (eq 5). The solvent shift can also be estimated by the approximation

$$\Delta E_{\mu}^{\text{perm}} \approx \Delta \Delta E_{\mu}^{\text{S}} + \sum_{\text{A}} \Delta Q_{\text{A}}^{\text{sf}} U_{\text{A}\mu}^{\text{perm}} = \Delta \Delta E_{\mu}^{\text{S}} + \Delta V_{\text{perm},\mu}^{\text{S}} \quad (12)$$

where  $\Delta \Delta E_{\mu}^{\text{S}}$  is the change in the solute contribution to the excitation energy as a result of the solute polarization by the solvent (see below) and  $\Delta Q_{\text{A}}^{\text{sf}}$  is the change of charge on atom A upon excitation. The last term in this expression gives the difference between the electrostatic solvation energies of the excited and the ground states. This expression does not reflect the energy invested in polarizing the solvent molecules since the energy is not released in the excited state. The energy involved in the solute polarization ( $\Delta \Delta E_{\mu}^{\text{S}}$ ) can be estimated by considering for the isolated solute and calculating the difference between the excitation energy where the molecular orbital vectors  $\psi$  are constrained to their values *in solution* (in the presence of  $U_{\mu}$ ) and the corresponding excitation energy where the  $\psi$ 's are relaxed to their gas-phase values. One may also try to estimate  $\Delta \Delta E_{\mu}^{\text{S}}$  by considering the solute as a classical polarizable dipole and noting that classically about half of the energy of interaction between an induced dipole and the corresponding inducing field is invested in polarizing the given dipole. This approximation gives

$$\Delta \Delta E_{\mu}^{\text{S}} \approx -\frac{1}{2} \sum_{\text{A}} [(Q_{\text{IA}}(U_{\mu}) - Q_{\text{IA}}(U=0))U_{\mu\text{A}} - (Q_{\text{BA}}(U_{\mu}) - Q_{\text{BA}}(U=0))U_{\mu\text{A}}] \quad (13)$$

This approximation, however, is somewhat questionable and is not examined in the present work. In the subsequent analysis, we shall consider only the energy  $E_{\mu 1}$  of the transition to the first excited state, since this is the most important channel in many photochemical reactions.

**2.2. Including the Induced Polarization of the Solvent.** In contrast to the simple treatment of hypothetical solvent systems with only permanent dipoles, one faces significant conceptual and practical difficulties in simulating electronic excitations in realistic solvents consisting of polarizable molecules. The electrons of the solvent atoms probably play an important role in the excitation process by responding instantly to the change in the solute electronic structure upon excitation. Describing this effect with the MO LCAO CI calculations of the solute electronic structure is not straightforward, since now the polarization part of the solvent potential is not fixed at its ground-state value. Perhaps the simplest consistent way to treat this problem is a second-order perturbation treatment of the solvent electronic states in the presence of the solute field (see Appendix). Such a treatment is equivalent to the classical consideration of the solvent induced dipoles,<sup>4b</sup> as long as we neglect the effect of the solvent excitations on the mixing between the solute states (see Appendix). Thus, we may write the solvation energy of a given solute charge distribution,  $Q^{\text{S}}$ , by the solvent induced dipoles as<sup>4b</sup>

$$\Delta E^{\text{ind}} = -\frac{1}{2} \sum_{\text{k}} m_{\text{k}}^{\text{ind}} \xi_{\text{k}}(Q^{\text{S}}) = \frac{1}{2} \sum_{\text{A}} Q_{\text{A}} U_{\text{A}}^{\text{ind}}(Q^{\text{S}}) \quad (14)$$

where  $m_{\text{k}}^{\text{ind}}$  and  $\xi_{\text{k}}$  are, respectively, the induced dipole of the  $k$ th solvent molecule and the local field at the corresponding site, while  $U_{\text{A}}^{\text{ind}}$  is the potential from the solvent induced dipoles.

Using eq 14 for the ground- and excited-state charge distributions of the solute molecule, as well as the ground-state polarization of the solvent permanent dipoles, we obtain

$$\Delta E_{\mu}^{\text{S}} = \Delta E_{\mu}^{\text{perm}} + \frac{1}{2} \sum_{\text{A}} (Q_{\text{A}\mu} U_{\text{A}\mu}^{\text{ind}} - Q_{\text{A}\mu} U_{\text{A}\mu}^{\text{ind}}) \quad (15)$$

Here  $\Delta E_{\mu}^{\text{perm}}$  is calculated with eq 11, and  $U_{\text{A}\mu}^{\text{ind}}$  and  $U_{\text{A}\mu}^{\text{ind}}$  are, respectively, the excited- and ground-state potentials from the induced solvent dipoles. The factor  $1/2$  accounts for the energy invested in the polarization of the solvent induced dipoles. This expression might be further manipulated in a simplified classical manner as

$$\Delta E_{\mu}^{\text{S}} = \Delta \Delta E_{\mu}^{\text{S}} + \sum_{\text{A}} (\Delta Q_{\text{A}}^{\text{sf}}) U_{\text{A}\mu}^{\text{perm}} + \frac{1}{2} \sum_{\text{A}} (Q_{\text{A}\mu} U_{\text{A}\mu}^{\text{ind}} - Q_{\text{A}\mu} U_{\text{A}\mu}^{\text{ind}}) = \Delta \Delta E_{\mu}^{\text{S}} + \Delta V_{\text{perm},\mu}^{\text{S}} + \Delta V_{\text{ind},\mu}^{\text{S}} \quad (16)$$

While the use of eq 16 is straightforward, it still presents a perturbation treatment, and one might look for alternative nonperturbative approaches. For example, we can try an approach, which seems in the first sight quite reasonable, and include  $U_{\mu}^{\text{ind}}$  in the solute Hamiltonian, using

$$F_{\mu\mu}^{\text{S}} = (F_{\mu\mu}^{\text{S}})_0 - U_{\text{A}\mu}^{\text{perm}} - U_{\text{A}\mu}^{\text{ind}} \quad (17)$$

The excitation energy associated with this procedure may be then evaluated by

$$\Delta E_{\mu}^{\text{S}} \approx (E_{\mu}^{\text{sol}}(U_{\mu}^{\text{perm}} + U_{\mu}^{\text{ind}}) - E_{\mu}^{\text{gas}}) - \sum_{\text{A}} \Delta Q_{\text{A}}^{\text{sf}} U_{\text{A}\mu}^{\text{ind}} + \frac{1}{2} \sum_{\text{A}} (Q_{\text{A}\mu} U_{\text{A}\mu}^{\text{ind}} - Q_{\text{A}\mu} U_{\text{A}\mu}^{\text{ind}}) \quad (18)$$

The  $\Delta Q_{\text{A}}^{\text{sf}}$  term is subtracted since the same term is implicitly included in  $E_{\mu}^{\text{sol}}$ , and it represents incorrectly the interaction between the solute charges and the solvent induced dipoles (this term gives an unphysical interaction between the solute excited-state charges and the solvent ground-state induced dipoles). After subtracting the  $\Delta Q_{\text{A}}^{\text{sf}}$  term, we are basically left with the same contribution as in eq 16 but now the solute polarization energy also involves the effect of  $U_{\mu}^{\text{ind}}$ , where the solute charges in both the ground and the excited states are influenced by  $U_{\mu}^{\text{ind}}$ . This approximation, however, is questionable, since the excited-state charges evaluated by using eq 17 with  $U_{\mu}^{\text{ind}}$  are not the correct excited-state charges (these charges should reflect  $U_{\mu}^{\text{ind}}$  in some way). One may suggest to solve for the excited state the equivalent of eq 17 with  $U_{\mu}^{\text{ind}}$  replacing  $U_{\mu}^{\text{ind}}$ . Such a treatment, however, will provide excited-state wave functions through a CI treatment that is not based on the same Hamiltonian used for the ground-state wave function. This involves wave functions that are not based on the variation principle. Of course, one may try to use for both the ground and the excited states a potential that is a linear combination of  $U_{\mu}^{\text{ind}}$  and  $U_{\mu}^{\text{ind}}$ , but it is not clear how to choose the optimal combination.

A possible way around the above problem might be provided by considering the effect of the solvent excitations on the interaction between the solute states (the corresponding off-diagonal elements are briefly discussed in the Appendix). Such a treatment is left, however, for subsequent studies, while in the present work we evaluate  $Q_{\mu}$  and  $Q_{\mu}$  using only  $U_{\mu}^{\text{perm}}$  (since this is consistent with the perturbation approach). While our actual calculations will be done with the approach of eq 15, it is still useful to have a first-order estimate for the solvent shift without considering the solute repolarization energy  $\Delta \Delta E_{\mu}^{\text{S}}$ . This estimate is obtained by

$$\Delta E_{\mu}^{\text{S}} = \sum_{\text{A}} \Delta Q_{\text{A}}^{\text{sf}} U_{\text{A}\mu}^{\text{perm}} + \frac{1}{2} \sum_{\text{A}} (Q_{\text{A}\mu} U_{\text{A}\mu}^{\text{ind}} - Q_{\text{A}\mu} U_{\text{A}\mu}^{\text{ind}}) = \Delta V_{\text{perm},\mu}^{\text{S}} + \Delta V_{\text{ind},\mu}^{\text{S}} \quad (19)$$

where the charges in this expression can be evaluated with or without the solvent potential.

To clarify the above discussion, we give in Figure 1 a schematic illustration of the different contributions to the solvent shift. The figure shows the interrelation between the orientations of the permanent dipoles and the polarization of the induced dipoles, demonstrating the fact that the excited-state induced dipoles of the solvent should respond to both the solute excited-state charges and the solvent ground-state permanent dipoles. Accounting consistently for such a complicated relationship by continuum models is quite a challenging problem (as long as the solute charge distribution cannot be described by the dipole approximation). This, however, is a straightforward task using a microscopic model of the type discussed in the next section.

**2.3. Implementation of Different Solvent Models in the Calculations.** The above derivation provided a general formulation without specific reference to the actual solvent model used. Our main point, however, is to have an explicit microscopic model that includes both permanent and induced dipoles. In the present work, we use both the simplified Langevin dipole (LD) model<sup>4a</sup> and the surface-constrained all atom solvent (SCAAS) model,<sup>14</sup> which will be briefly described below.

**2.3.1. Calculations of Absorption Spectra in Solution Using the LD Model.** Probably the simplest microscopic model that can give reliable spectra for molecules in solution is the LD model. This model represents the solvent molecules by a cubic grid with permanent and in some cases (e.g., ref 4a) induced components. The field on each dipole is determined self-consistently by considering the field from both the solute and the other solvent dipoles. The projection of the solvent permanent dipoles on the direction of their local field is approximated by a Langevin-type formula.

$$m_{\text{k}}^{\text{perm},n+1} = e_{\text{k}} m_{\text{k}} \left( \coth X_{\text{k}}^n - \frac{1}{X_{\text{k}}^n} \right) \quad k = 1, N \quad (20)$$

$$X_{\text{k}} = \frac{m_{\text{k}} \xi_{\text{k}}^n}{k_{\text{B}} T d(r_{\text{k}})}$$

(14) (a) Warshel, A.; King, G. *Chem. Phys. Lett.* **1985**, *121*, 124. (b) King, G.; Warshel, A. *J. Chem. Phys.* **1989**, *91*, 3647.

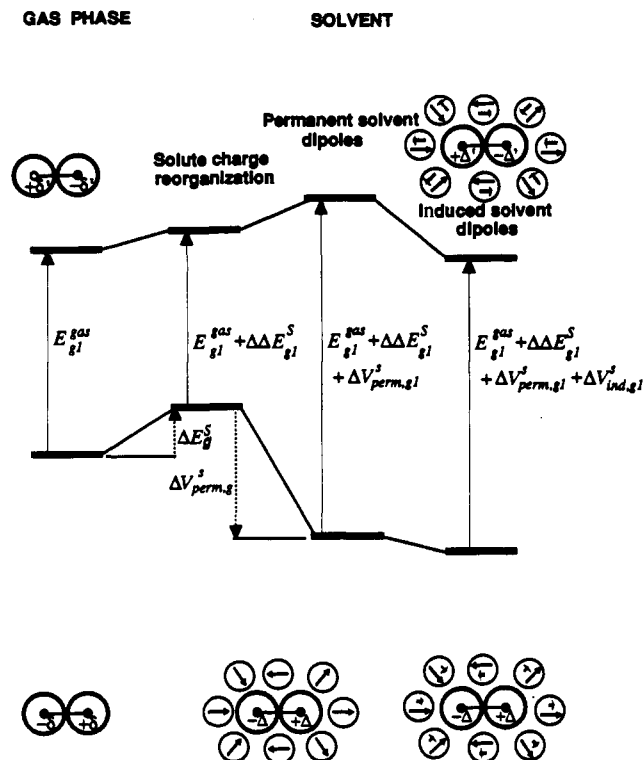


**Figure 1.** Schematic description of the effect of the solvent on electronic excitation. The figure describes the solute in its ground- and excited-state charge distributions, where  $\delta$  and  $\Delta$  are, respectively, the corresponding partial charges with and without the inclusion of the solvent permanent and induced dipoles in the solute's Hamiltonian (the notations  $\delta'$  and  $\Delta'$  are used for the excited-state charges). The solvent permanent and induced dipoles are described by the dark and light arrows, respectively. The notations used for the different contributions are given in the text. In considering the figure, it is useful to examine first the effect associated with the solvent permanent dipoles (this involves both  $\Delta V_{perm}^S$  and the energy associated with the corresponding solutes' charge redistribution,  $\Delta E_g^S$ ). As illustrated in the figure, about half of the energy gained from the stabilization of the solutes' ground state by the solvent permanent dipoles is invested in polarizing the solute ( $\Delta E_g^S = -1/2 V_{perm,g}^S$ ). The combined effect of  $\Delta\Delta E_{g1}^S$  and  $\Delta V_{perm,g1}^S$  constitutes the effect of the solvent permanent dipoles. The effect of the solvent induced dipoles is depicted in the right-hand side of the figure. This effect is much larger in the excited state than in the ground state. This is due to the fact that the ground-state charges are already stabilized by the solvent permanent dipoles, which screen the solute's field from the solvent induced dipoles. In the excited state, on the other hand, the solvent permanent dipoles are frozen in their ground-state polarization, which destabilizes the solute charge distribution. Thus, the induced dipoles have now the opposite polarization to that of the permanent dipoles and much larger effect in stabilizing the solute charges.

where  $m_0$  is the solvent dipole moment and  $\xi_k^n$  is the electric field on the  $k$ th solvent dipole from the solute charge distribution and all the other solvent permanent dipoles in the  $n$ th iteration.  $e_k$  is a unit vector in the direction of  $\xi_k$ ,  $N$  is the total number of solvent dipoles,  $d(r_k)$  is a screening function that represents the attenuation of the solute field on the  $k$ th dipole by the field from the other solvent molecules (where  $r_k$  is the distance between the solvent and the closest solute atom). The initial value of  $\xi_k$  in the iterative procedure of eq 20 is taken as the field from the solute charges. Usually  $d(r)$  is taken as unity in iterative treatments. However, we found here that similar results and faster convergence can be obtained with  $d(r) = r - 2$ , which is usually used in noniterative treatments.<sup>4b</sup>

The induced dipoles  $m_k^{ind}$  are calculated after evaluating the permanent dipoles, with use of

$$m_k^{ind} = \alpha \xi_k \quad (21)$$

where  $\alpha$  is the average polarizability of the solvent molecule and  $\xi_k$  is the field from the solute as well as the permanent and induced dipoles of the other solvent molecules. The total polarization of each solvent dipole is taken now as the sum of the corresponding permanent and induced components. However, as discussed in section 2.2, we calculate the

**Table I.** Parameters Used in the LD Solvent Model<sup>a</sup>

| parameter <sup>a</sup>                         | Solvent Point Dipole Descriptors |          |
|--|----------------------------------|----------|
|  | polar                            | nonpolar |
| van der Waals radii, Å                         | 1.50                             | 1.90     |
| dipole moment ( $m_0$ ), D                     | 1.85                             | 0.00     |
| polarizability ( $\alpha$ ), Å <sup>3</sup>    | 1.45                             | 1.84     |
| grid spacing ( $\Delta$ ), Å                   | 3.10                             | 3.10     |
| grid radius ( $R_g$ ), Å                       | 12–19                            |          |
| Solute Atomic van der Waals Radii <sup>b</sup> |                                  |          |
| atom   | $R_w$ , Å                        |          |
| H  | 1.2                              |          |
| C  | 2.0                              |          |
| N  | 1.4                              |          |
| O  | 1.3                              |          |

<sup>a</sup> The parameters for polar and nonpolar solvents are chosen according to the experimental data<sup>13</sup> for water and hydrocarbon media, respectively. <sup>b</sup> The closest distance of the solvent dipoles to the solute atoms is given by the sum of the solute and solvent van der Waals radii (i.e.,  $R_w + 1.5$ ).

excitation energies considering the effect of the induced dipoles through a perturbation treatment. This means that the solutes' SCF equation is evaluated while considering only the potential from the solvent permanent dipoles. That is, the SCF equation for the LD solvent model is taken as

$$(F_{\mu\mu}^S)^{(n)} = (F_{\mu\mu})_0 - \sum_k (m_k^{perm})^{(n-1)} r_{kA} / r_{kA}^3 \quad (22)$$

where the index  $n$  indicates that we are dealing with an iterative procedure that considers the self-consistent interaction between the solute's ground-state charges and the solvent permanent dipoles (the Langevin dipoles).

In our quantum chemical studies, the chromophore is surrounded by the above-mentioned grid of point dipoles. The solvent dipoles in the first solvation shell are distributed around the solute in a special procedure (see below), while the rest of the solvent dipoles are situated on a regular cubic grid, which is extended around the center of the chromophore up to a radius,  $R_g$ , of typically 16 Å. The grid is then surrounded by a bulk solvent, which is treated as a dielectric continuum.<sup>4b</sup>

The coordinates of the dipoles in the first solvation shell are generated by the following procedure. (i) A dense grid of 1-Å spacing is built around the solute, deleting all points whose distance from the closest solute atom is smaller than the sum of the corresponding solute and solvent van der Waals radii (see Table I for the relevant parameters). (ii) The dense grid is converted to a surface by deleting any point that is more than 4 Å from the closest solute atom. (iii) The spacing of the resulting solvation envelope is now increased to the standard spacing,  $\Delta$ , expected from the given solvent (e.g., 3.1 Å for water). This is done by deleting grid points that are within a distance of less than  $\Delta$  from their neighbors. The resulting solvation envelope is surrounded by a regular cubic grid, whose points are separated by  $\Delta$  from each other and by a distance larger or equal to  $\Delta$  from any point on the solvation envelope. The solvation energy and the relevant  $U_g$  associated with the given solute ground-state charges are then obtained by averaging over several grid configurations (typically 4–6 configurations).

The parameters of the LD solvent model are given in Table I. Here we use the experimental values of the molecular dipole moments and polarizabilities for water and hydrocarbon (for the  $-\text{CH}_2-$  group) solvents<sup>13</sup>. The spacing of the cubic grid is estimated from the experimental data on the molar density of water and  $-\text{CH}_2-$  groups for aliphatic hydrocarbons.<sup>13a</sup> The values of atomic van der Waals radii,  $R_w$ , are parametrized by fitting the calculated and observed solvation energies of the ground states of different molecules and ions. In the calculations of  $U_g$  for nonpolar solvents, each  $\text{CH}_2$  group is modeled with its own dipole. Here we use the  $m$ 's of eq 21 with a grid spacing of 3.10 Å and with  $\alpha = 1.84 \text{ Å}^3$ , which corresponds to the average polarizability of a  $-\text{CH}_2-$  group.<sup>13b</sup> This gives, with the Clausius–Mossotti relationship, a macroscopic dielectric constant of  $\epsilon = 2.04$ .

The electronic structure of the solute is calculated with the quantum mechanical extension of the Consistent Force Field to conjugated molecules (QCFF/PI) (e.g., see ref 15) by using the heteroatoms version of ref 7. This method is based on a formal separation of  $\sigma$  and  $\pi$  electrons, with the former represented by analytical empirical potential functions

(15) Warshel, A. In *Semiempirical Methods of Electronic Structure Calculation*; Segal, G. A., Ed.; Plenum Press: New York, 1977.

**Table II.** Calculated and Observed Solvent Effects on the First  $\pi \rightarrow \pi^*$  Transition of Acrolein (1), Mesityl oxide (2), and Retinal (3)<sup>a</sup>

| N | method   | polar           |                  |                         |                     | nonpolar           |                         | differential solvent shift <sup>b</sup> |               |                   |
|---|----------|-----------------|------------------|-------------------------|---------------------|--------------------|-------------------------|---|---------------|-------------------|
|   |          | $E_{g1}^{obsd}$ | $E_{g1}^{calcd}$ | $\Delta E_{g1}^{calcd}$ | $\Delta V_{perm}^s$ | $\Delta V_{ind}^s$ | $\Delta E_{g1}^{calcd}$ | $\Delta V_{ind}^s$                      | calcd         | obsd <sup>c</sup> |
| 1 | perm     |                 | 43 700           | -2819                   | -1652               |                    |                         |   | -2819 (-1652) |                   |
|   | perm+ind |                 | 43 248           | -3270                   | -1652               | -451               | -315                    | -315                                    | -2955 (-2073) |                   |
|   | perm,ind |                 | 42 735           | -3888                   | -1855               | -511               | -981                    | -394                                    | -2907 (-1973) |                   |
| 2 | perm     |                 | 42 493           | -1899                   | -1630               |                    |                         |   | -1899 (-1630) |                   |
|   | perm+ind | 41 220          | 41 984           | -2408                   | -1630               | -509               | -340                    | -340                                    | -2068 (-1799) | -2145             |
|   | perm,ind |                 | 41 603           | -2777                   | -1728               | -541               | -715                    | -380                                    | -2062 (-1348) |                   |
| 3 | perm     |                 | 26 948           | -642                    | -1328               |                    |                         |   | -642 (-1328)  |                   |
|   | perm+ind | 26 450          | 26 608           | -1582                   | -1328               | -941               | -716                    | -716                                    | -866 (-1522)  | -702              |
|   | perm,ind |                 | 25 570           | -1990                   | -1609               | -1095              | -1008                   | -857                                    | -982 (-1846)  |                   |

<sup>a</sup>Energies (cm<sup>-1</sup>) calculated with the QCFF/SOL (LD) program. The calculations were done with eqs 11, 15, and 17, which are referred to, respectively, as "perm", "perm+ind" and "perm,ind". The excitation energies,  $E_{g1}^{obsd}$ , correspond to the spectra in water for mesityl oxide<sup>20</sup> and in ethanol for retinal.<sup>21a</sup> <sup>b</sup>The differential solvent shift represents the difference in solvent shift between polar and nonpolar solvents. The calculated value in brackets designates the corresponding classical shift of eq 19 (the change in the relevant  $\Delta V^s$ ). <sup>c</sup>The observed differential solvent shift for mesityl oxide is taken as the difference between the absorption maxima in water and in isooctane.<sup>20</sup> The observed solvent shift for retinal is taken as the difference between the absorption maxima at room temperature in ethanol<sup>21b</sup> and in PMh<sup>21b</sup> (a 5:1 mixture of 2-methylbutane and methylcyclohexane); the shift relative to water is expected to be somewhat larger.

and the latter by a second-order analytical representation of a Pariser-Parr-Pople-type model, corrected for orbital overlap. This approach provides both ground- and excited-state potential surfaces for conjugated hydrocarbons as well as other heteroatomic molecules with delocalized  $\pi$  electrons. The extensive parametrization of the method allows one to obtain reliable results for a wide class of molecular properties, including equilibrium geometries, vibrational spectra, ionization energies, and electronic spectra (see ref 15). The incorporation of the potential from the LD solvent model in the QCFF/PI Hamiltonian can be conveniently done via eq 22, and the corresponding solvent shift can be evaluated with eq 15. The program package that incorporates various solvent models in the QCFF/PI quantum chemical calculations is called the QCFF/SOL program and is a part of the package MOLARIS.<sup>16</sup>

**2.3.2. Calculations of Absorption Line Shapes by Using the SCAAS Model.** Although the LD model provides a very convenient way of obtaining solvent effects on absorption spectra, it is important to explore more explicit solvent models. In this work, we examine calculations of solvent shifts using the Surface-Constrained All Atom Solvent (SCAAS) model. This model has been introduced before<sup>14</sup> and is an extension of our earlier surface-constrained dipolar models.<sup>4,9</sup> The SCAAS model represents explicitly all the solvent atoms, by using a standard force field with van der Waals and electrostatic terms as well as intramolecular terms.<sup>14</sup> The model involves spherical boundary conditions that constrain the molecules on the surface of the finite simulation system (usually  $\sim 100$  solvent molecules) to have the same polarization as they would have in an infinite solvent system (for more details, see ref 14 and, for earlier related models, see ref 4).

The incorporation of the SCAAS model in the solute Hamiltonian is conveniently done with eq 5. However, the main difference from the LD treatment is that now we include in eq 5 the potential associated with the instant solvent configuration and evaluate the average of the calculated excitation energies (rather than using the average solvent polarization in a single calculation of the excitation energy). That is, in order to obtain the relevant excitation energy, we ran trajectories of the solute-solvent system, where the intermolecular forces in each MD step correspond to the solute's ground-state charges that reflect the potential from the solvent in the configuration obtained from the previous MD step. Solving the corresponding CI equation at each MD step, we obtain the Boltzmann average excitation energy by

$$\Delta E_{gf} = \frac{1}{N} \sum_i^N \Delta E_{gf}(t_i) \quad (23)$$

where  $t_i$  is the  $i$ th MD time steps and where we exploit the ergodic hypothesis, replacing the configuration average by the time average over a long trajectory. Equation 23 includes the effect of the solvent induced dipoles by evaluating the correction term of eq 15 at each step of the trajectory. This requires, of course, to have a water model with induced dipoles, which is accomplished by using the appropriate SCAAS model.<sup>14</sup>

Another more rigorous variant of the calculations is obtained with the dispersed polaron model.<sup>11</sup> In this model, which is described in detail

elsewhere,<sup>11</sup> we evaluate the line shape of the given electronic transition by<sup>17</sup>

$$I(\omega_0) = B \mu_{gf}^2 \int_{-\infty}^{+\infty} \exp[i\omega_{gf}t + \gamma(t)] dt \quad (24)$$

where  $\mu_{gf}$  is the transition dipole,  $B$  is a constant and  $\omega_{gf}$  is given by

$$\omega_{gf} = (\Delta E_{gf})_g / \hbar - \omega_0 \quad (25)$$

Here  $( )_g$  designates an average over trajectories on the ground-state potential surface,  $\hbar\omega_0$  is the light energy, and the function  $\gamma$  is given by

$$\gamma = \sum_j \Delta_j^2 [(\bar{n}_j + 1/2)(\cos \omega_j t - 1) + i \sum_j (\Delta_j^2 / 2) \sin \omega_j t] \quad (26)$$

Here  $\Delta_j$  and  $\omega_j$  are, respectively, the dimensionless coordinate displacement (origin shift) and frequency of the  $j$ th solvent mode and  $\bar{n}_j$  is given by

$$\bar{n}_j = 1 / [\exp(\hbar\omega_j / k_B T) - 1] \quad (27)$$

The  $\Delta_j$ 's are evaluated from the amplitudes,  $A(\omega)$ , of the power spectrum of  $\Delta E(t) - \langle \Delta E \rangle_g$  by using the relationship<sup>11</sup>

$$\lim_{\tau \rightarrow \infty} |A(\omega)|^2 / \tau = \pi \hbar \omega k_B T \sum_j \Delta_j^2 \delta(\omega - \omega_j) \quad (28)$$

where  $\tau$  is the finite time used in evaluating this power spectrum and where  $A(\omega)$  is subjected to the normalization.

$$\int_{-\infty}^{+\infty} (|A(\omega)|^2 / \tau) d\omega = 2\pi ((\Delta E_{gf})_g - \Delta E_{gf}^0) k_B T = 2\pi \lambda k_B T \quad (29)$$

where  $\Delta E_{gf}^0$  is the difference between the minima of  $E_g$  and  $E_f$ . The parameter  $\lambda$  is referred to as the "reorganization energy". The derivation of the above expressions is given in ref 11 for the rate constant of transfer between two electronic surfaces in solution, and the generalization to absorption of light is based on considering this process as a crossing between a state of the ground state plus the light energy  $\hbar\omega_0$  and the excited electronic state (see refs 17 and 18).

### 3. Results and Discussion

**3.1. Calculations of Spectral Properties of Polyene Aldehydes in Solutions.** To examine the approaches developed in the previous section, we calculated the solvent effect on the spectra of three molecules with a well-defined strong first  $\pi \rightarrow \pi^*$  transition:

(17) (a) Warshel, A.; Stern, P. S.; Mukamel, S. *J. Chem. Phys.* **1983**, *78*, 7498. (b) Warshel, A.; Stern, P. S.; Mukamel, S. In *Time-Resolved Vibrational Spectroscopy*; Atkinson, G. H., Ed.; Academic: New York, 1983; p 41.

(18) Warshel, A.; Hwang, J.-K. *J. Chem. Phys.* **1985**, *82*, 1756.

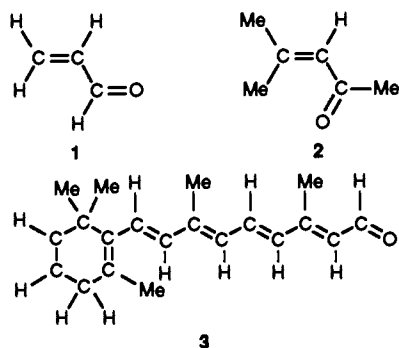
(19) Hwang, J.-K.; Warshel, A. *J. Am. Chem. Soc.* **1987**, *109*, 715.

(20) Kosower, M. E. *J. Am. Chem. Soc.* **1958**, *80*, 3261.

(21) (a) Moore, T. A.; Song, P.-S. *Nature (London)*, **1973**, *243*, 30. (b) Sperling, W. S. In *Biochemistry and Physiology of Visual Pigments*; Langer, H., Ed.; Springer-Verlag: New York, 1973; p 19.

(16) Warshel, A.; Creighton, S. In *Computer Simulation of Biomolecular Systems*; van Gunsteren, W. F., Weiner, P. K., Eds.; ESCOM: Leiden, 1989; p 120.

acrolein (1), mesityl oxide (2), and retinal (3). Molecules 1 and 3 were considered in the all-trans conformation, while 2 was considered in its more stable cis conformation. The results of



the calculated excitation energies in different approximations, the spectral shifts associated with transfer from polar to nonpolar solvents, and the available experimental data are given in Table II. The calculated values of the first  $\pi \rightarrow \pi^*$  transition,  $E_{g1}$ , in polar media reproduce fairly well the experimental energies in water (Table II). In all cases, the calculations predict correctly a red shift between the spectra in polar and nonpolar media. Both the  $\Delta E_{g1}$  and the corresponding solvent shifts decrease with the increase of the size of the molecule.

In considering the influence of the solvent on the excitation energies of our three molecules, let us consider first the classical picture of the solute-solvent interactions. The largest calculated  $\Delta Q_A^{\text{st}}$  for all three compounds involves the migration of a negative charge to the C atom next to the O atom. For example, in 1 this charge increment is 0.38 eu, while the charge of the O atom remains practically unchanged. The overall effect of the  $\pi \rightarrow \pi^*$  excitation is an increase of the dipole moment of the excited state (for 1 from 4.1 to 7.0 D) with a conservation of its space orientation. For the latter reason, the equilibrium polarization of the permanent solvent dipoles around the solute in the ground state would also stabilize the excited state but to a greater extent since the solute dipole increases. The induced solvent dipoles also stabilize the excited-state solute dipole more than they stabilize the smaller ground-state dipole. Thus, the increase in the solute polarity and the conservation of the orientation of the solute dipole lead to greater stabilization of the excited state by both the permanent and induced solvent dipoles. This leads to a red shift of  $E_{g1}$  in solutions relative to the gas phase, and the shift should be greater in polar solvents than in nonpolar solvents. The magnitude of the change in dipole moment upon excitation decreases in the order 1 > 2 > 3, and the corresponding solvent shifts decrease in the same order (see Table II).

Although the largest contribution to the solvent shift in the above example is associated with the permanent dipoles contribution ( $\Delta V_{\text{perm}}^{\text{st}}$ ), the induced dipoles contribution ( $\Delta V_{\text{ind}}^{\text{st}}$ ) is also significant, contributing between 30 and 50%. However, the contribution of induced dipoles to the solvation energies of the ground state are only around 10–15% of the corresponding permanent dipoles term. This indicates that, in polar solvents, the induced dipoles play a more important role in stabilizing excited states than they do in stabilizing ground states (a possible exception might occur if the excited-state dipole of the solute is very small). In nonpolar media,  $\Delta E_{g1}$  is obviously associated only with the  $V_{\text{ind}}^{\text{st}}$  terms. However, in the present test case, the induced dipole contributions in polar and nonpolar solvents are similar and the corresponding difference in spectral shift is largely determined by the  $\Delta V_{\text{perm}}^{\text{st}}$  term.

Despite the instructive trend obtained from the classical considerations, it is important to note the large difference between the quantum chemical value  $\Delta E_{g1}$  and the classical solvent contribution  $\Delta V_{\text{perm}}^{\text{st}} + \Delta V_{\text{ind}}^{\text{st}}$ . This indicates the importance of the  $\Delta \Delta E^{\text{st}}$  term and shows that a reliable estimate of  $\Delta E_{g1}$  can not be obtained by considering only the solvation energies of the ground and excited states (as was done in the previous studies<sup>1,2</sup>). That is, the inclusion of  $U_{\text{g}}^{\text{perm}}$  in the solute Hamiltonian and the

Table III. Calculated and Observed Solvent Effects for the First  $\pi \rightarrow \pi^*$  Transition in Merocyanine Dyes 4 and 5<sup>a</sup>

| N | form | polar    |                 | nonpolar |          | differential solvent shift |                        |       |
|---|------|----------|-----------------|----------|----------|----------------------------|------------------------|-------|
|   |      | $E_{g1}$ | $\Delta E_{g1}$ | form     | $E_{g1}$ | $\Delta E_{g1}$            | calcd                  | obsd  |
| 4 | a    | 20 535   | -703            | a        | 21 873   | 212                        | 3826 <sup>(a-b)</sup>  |       |
|   | b    | 25 699   | 6820            | b        | 20 959   | 2080                       | 4740 <sup>(b-a)</sup>  | 6079  |
| 5 | a    | 22 888   | -3561           | a        | 26 023   | -630                       | -3135 <sup>(a-a)</sup> | -3146 |
|   | b    | 20 270   | -1984           | b        | 22 427   | 174                        | -2157 <sup>(b-b)</sup> |       |

<sup>a</sup> Energies ( $\text{cm}^{-1}$ ) calculated with the QCFF/SOL (LD) program by using eq 15. The differential solvent shift represents shift obtained upon transfer of the indicated molecule from a nonpolar to polar solvent. The corresponding shift is evaluated with the resonance forms indicated in parentheses. Thus, for example, we evaluate the shift for 4 by using the eno form b for the polar solvent and the keto form a for nonpolar solvent. This reflects the assumed structure in each case. The observed solvent shift is taken as the difference between the absorption maxima in water and in pyridin<sup>23a</sup> for molecule 4<sup>23a</sup> and as the difference between the absorption maxima in water and cyclohexane for molecule 5.<sup>23b</sup>

resulting evaluation of the solute polarization energy are essential for reliable calculations of solvent shifts. A related point has been made before with regard to ground-state calculations.<sup>22</sup>

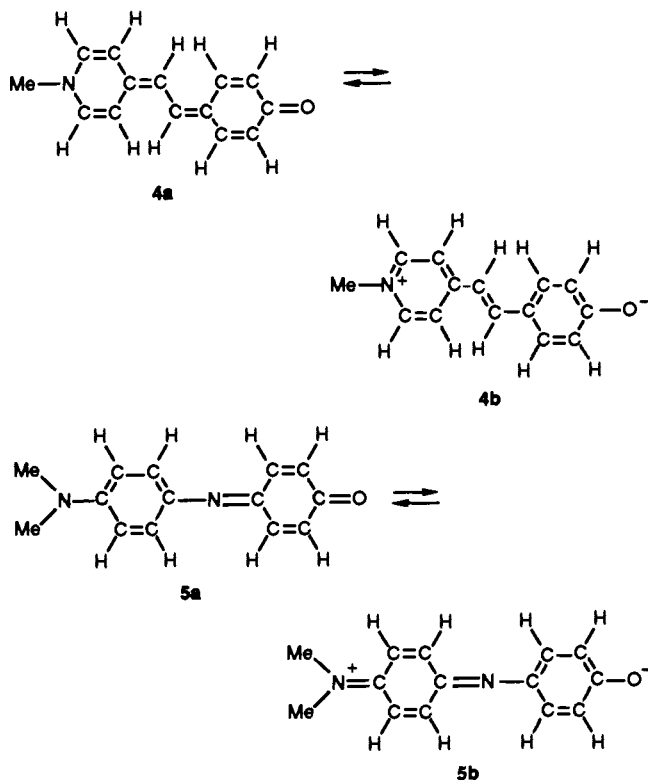
The dependence of the calculated  $\Delta E_{g1}$  on the method used is demonstrated in Table II, which compares the results obtained with eqs 11, 15, and 17 (which are referred to, respectively, as methods "perm", "perm+ind", and "perm,ind"). The calculated solvent shift increases when the effect of the induced dipoles is considered (i.e., by using eqs 15 and 17). For 2 and 3, the values of the differential solvent shift between polar and nonpolar solvents agree well with the experimental shift when eq 15 is used. The calculated  $\Delta E_{g1}$ 's reach their largest values when eq 17 is used, but when one considers the difference in solvent shifts between polar and nonpolar media, this additional induced dipole effect is largely canceled out and the calculated values of the solvent shift are almost the same for the perm+ind and perm,ind methods (eqs 15 and 17, respectively).

**3.2. Calculations of the Spectral Properties of Merocyanine Dyes.** The merocyanine dyes display remarkable sensitivity to the polarity of the solvent and present an excellent test case for the calculations of solvent shifts. Here we have chosen two compounds (dyes 4 and 5) whose spectral properties were studied by Brooker et al.<sup>23</sup> Dye 4 shows a large blue solvent shift when transferred from nonpolar to polar media, and dye 5 displays a large red shift. Unlike the previous case with polyene aldehydes, which have almost the same geometry in polar and nonpolar solvents, the merocyanine molecules have an alternating bond character, which can vary between the two extreme keto-like and eno-like resonance forms (which are referred to here as "keto" and "eno"). The large variations in absorption spectra are believed to be associated with the existence of the molecules in either the neutral keto or the ionic eno resonance forms in different solvents. The results of calculations of spectral properties of each of those forms are given in Table III.

It is important to comment at this point about the procedure used to obtain the geometries for the spectral calculations. Using the QCFF/PI program for a standard geometry optimization of both dyes yields structures with bond lengths characteristic of the keto forms 4a and 5a, even when the solvent effect is included. Apparently, the QCFF/PI as well as other semiempirical methods underestimates the stability of the eno form relative to the keto form, and the same is true for any other ion pair type configurations. This may be due in part to the fact that the semiempirical repulsive integrals are smaller than the corresponding ab initio integrals.<sup>24</sup> This problem could be corrected by using larger  $\gamma$ 's,

(22) Hwang, J.-K.; King, G.; Creighton, S.; Warshel, A. *J. Am. Chem. Soc.* **1988**, *110*, 5297.

(23) (a) Brooker, L. G. S.; Keyes, G. H.; Heseltine, D. W. *J. Am. Chem. Soc.* **1951**, *73*, 5350. (b) Brooker, L. G. S.; Craig, A. C.; Heseltine, D. W.; Jenkins, P. W.; Lincoln, L. L. *J. Am. Chem. Soc.* **1965**, *87*, 2443.



but in the present work we choose to delay the corresponding reparametrization effort (which is not related to the calculations of the solvent spectral effects) and to use a valence bond type philosophy in evaluating the relevant eno structures (see ref 25 for a related effort). This was done by minimizing the structure of the eno molecules in two steps, one with the isolated phenoxy ion and one with the positive ion fragment formed by removing the phenoxy group from the molecule. Connecting the two minimized fragments provides the structure for the spectral calculations of the eno molecule. Using this geometry, we find that the calculated  $\pi$ -electron distribution in the eno forms of **4b** and **5b** in polar solvents resembles the charge distribution of the corresponding VB resonance formulas. The calculations give a large negative charge on the O atom and a positive charge that is delocalized over the whole aromatic system. The dipole moment of **4b** is larger than that of **5b**, as is apparent from the corresponding change in solvation energies ( $-67.7$  and  $-31.7$  kcal/mol for **4b** and **5b**, respectively). The intramolecular charge separation in the keto forms of **4** and **5** is smaller than in the eno forms, and the corresponding solvation energies have lower values ( $-48.1$  and  $-13.3$  kcal/mol for **4a** and **5a**, respectively). This reference gas-phase calculations of the electronic structures of **4** and **5** give, in all cases, the keto electronic configuration (which is characterized by a small degree of charge separation between the O and N atoms).

In the excited state, the polarity of both forms of **4** decreases, due to migration of electron density from the O atom to the aromatic system. This results in a lower solvent stabilization of the excited state of the dye and, consequently, a blue shift in the spectra due to the  $\Delta V_{\text{perm}}^s$  term. The calculations for **5** have produced an increase in the excited-state charge separation due to the migration of a negative charge to the N azine atom. The corresponding change of the  $\Delta V^s$  term accounts for the red shift in the spectra of **5**.

(24) The semiempirical  $\gamma_{\mu\nu}$ 's (which are calibrated by using spectral properties) are much smaller than the corresponding ab initio integrals. This might be due to the fact that the semiempirical methods do not account for the stabilization of excited-state charges by repolarization of the inner core electrons. Such an effect, which could have been modeled by using induced dipoles to represent the inner shell electrons, is inconsistently accounted for by using small  $\gamma$ 's.

(25) Warshel, A.; Deakyne, C. *Chem. Phys. Lett.* 1978, 55, 459.

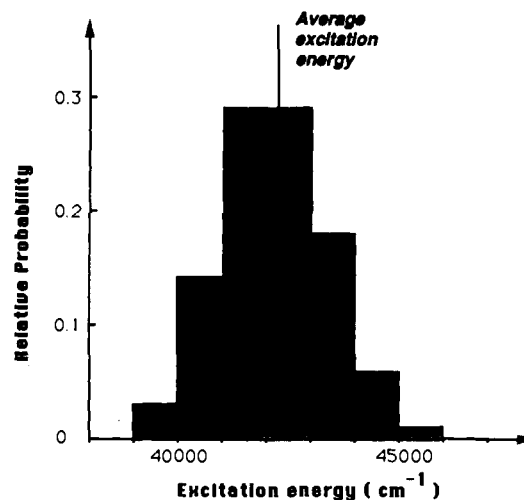


Figure 2. Calculated distribution of the excitation energy  $E_{g1}$  of mesityl oxide in a polar solvent obtained with the SCAAS model. Each bar represents the relative number of points along the MD trajectory having a given value of  $E_{g1}$  within an interval of  $1000 \text{ cm}^{-1}$ . The calculated average value of  $E_{g1}$  is  $42118 \text{ cm}^{-1}$ .

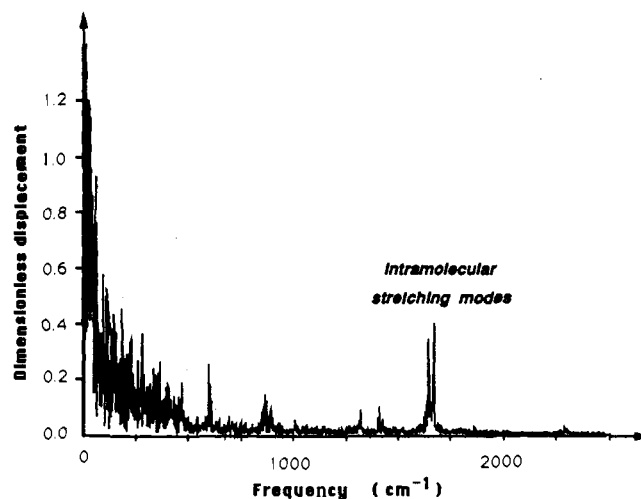
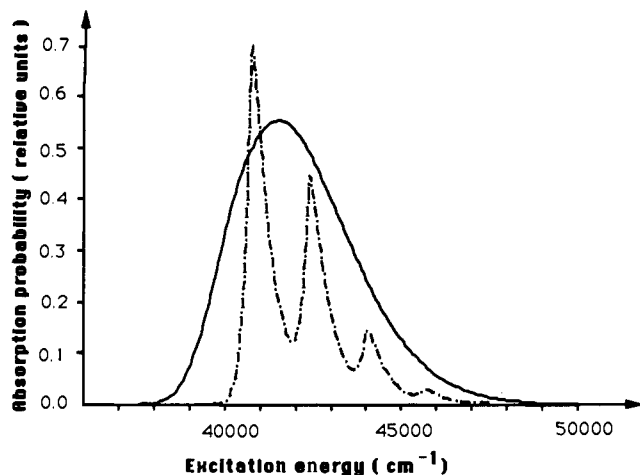


Figure 3. Dimensionless origin shifts  $\Delta(\omega)$  obtained by the dispersed polaron approach for the  $\Delta E_{g1}$  of mesityl oxide in the SCAAS solvent model.

In solution, the structure of merocyanine dyes could change within the limits of the quite different geometries of the eno and keto forms. The shift of the structure toward either of these forms should depend in a complicated manner upon the properties of the solvent. According to experimental observations,<sup>22</sup> dye **4** is much more polar than **5**. Thus, one can expect that **4** would exist in the form **b** in a polar solvent but would have contributions from both forms **a** and **b** in a nonpolar solvent. For the weakly polar dye **5**, the structure in a polar solvent should be given by a combination of forms **a** and **b**, while in nonpolar, predominantly by form **a**. As can be seen from Table III, the calculated values of  $E_{g1}$  and  $\Delta E_{g1}$  depend greatly upon the given geometry and the corresponding charge distribution of **4** and **5**. The experimentally observed solvent shifts between polar and nonpolar media could be best reproduced if **4** is assumed to be in form **b** in both polar and nonpolar solvent and if **5** is taken to be in form **a** both in polar and nonpolar solvents. Considering the uncertainty of the structure of molecules **4** and **5** in different solvents, it appears that our calculated solvent shifts reproduce fairly well the qualitative features of the corresponding observed spectral shifts of these merocyanine dyes.

**3.3. SCAAS/MD Simulations of Solvent Shift in Mesityl Oxide.** In addition to using the QCFF/SOL (LD) approach, we examined the absorption spectra of mesityl oxide (**2**) with the more rigorous SCAAS model and the MD simulation approach of section 2.3.2.



**Figure 4.** Dispersed polaron line shape for the first  $\pi \rightarrow \pi^*$  transition of mesityl oxide, obtained with the  $\Delta(\omega)$  of Figure 3 and eq 24. The solid curve represents the line shape obtained with  $\lambda_s = 3.0$  and  $\lambda_s = 6.0$  kcal/mol. The dashed curve represents the line shape obtained with  $\lambda_s = 3.0$  and  $\lambda_s = 1.0$  kcal/mol.

The MD simulation was performed with a system composed of the solute **2** and 243 water molecules, confined to a sphere of 12-Å radius whose surface molecules satisfy the SCAAS surface constraints.<sup>14</sup> The calculations involved a 5-ps relaxation followed by a 25-ps simulation period. The QCFF/SOL SCF CI excitation energy was collected every 10 MD steps. This was done for both the solvated solute and the isolated solute, giving the  $\Delta E_{g_1}^{\text{perm}}$  of eq 11. The effect of the induced dipoles was also evaluated every 10 steps and added to  $\Delta E_{g_1}^{\text{perm}}$  to give the  $\Delta E_{g_1}$  of eq 15. The histogram showing the distribution of the computed excitation energies for this system is given in Figure 2. These energies range from 39 000 to 45 000  $\text{cm}^{-1}$  with an average of 42 118  $\text{cm}^{-1}$ , and the corresponding average of  $\Delta E_{g_1}^{\text{sol}}$ , evaluated through eq 23, is 2293  $\text{cm}^{-1}$ .

Preliminary calculations of the absorption line shape of mesityl oxide were also performed with the SCAAS model and the dispersed polaron treatment of section 2.3. The reorganization energy term of eq 29 was estimated from the sum of the solvent and the solute reorganization energies. The solvent reorganization energy was conveniently estimated with the QCFF/SOL (LD) approach as the difference between the solvation energy of the unrelaxed excited state (with the ground-state permanent dipoles) and the excited state with relaxed solvent dipoles. The induced solvent dipoles were allowed to reorient self-consistently in response to the solute and solvent permanent charges. The resulting *solvent* reorganization energy ( $\lambda_s$ ) for mesityl oxide in a polar solvent is 6.0 kcal/mol. The solute reorganization energy was approximated by the difference between the energies of the unrelaxed and relaxed excited-state geometries of the solute. This procedure gave a *solute* reorganization energy ( $\lambda_s$ ) of 3.0 kcal/mol for mesityl oxide. A more rigorous estimate could have been obtained by the free energy perturbation approach of ref 19, but this requires more computer time for convergence.

Using the above reorganization energy to normalize the power spectrum of the  $\Delta E_{g_1}$  of our system, we obtain the dependence of  $|A(\omega)^2/\omega|$  on  $\omega$ , and the corresponding origin shifts (the  $\Delta$ 's of eqs 26 and 28) are given in Figure 3. Using these results in eq 26 and substituting in eq 24, we obtained the line shape presented in Figure 4. The calculations produce a structureless line shape not much different than the corresponding observed spectrum. Figure 4 also presents the calculated spectrum obtained by using a smaller solvent reorganization energy ( $\lambda_s = 1.0$  kcal/mol). As could be expected, we see a vibronic progression in the spectrum.

More studies are clearly needed, and particular attention should be given to the change in the line shape upon change in the solvent and temperature. However, the present study demonstrates that such calculations are feasible. It is also instructive to note that

the LD solvent shift and the corresponding SCAAS shift are quite similar (2068 and 2293  $\text{cm}^{-1}$ , respectively).

#### 4. Concluding Remarks

This work developed and examined practical approaches for calculations of solvent effects on electronic spectra. The methods developed include a variant of our early LD approach and an all-atom MD approach. Both approaches incorporate the solvent consistently in the solute Hamiltonian and take into account the solvent induced dipoles. The calculations reproduce the observed solvent effect on several well-defined test cases of polyene aldehydes and merocyanine dyes. The present study differs from previous phenomenological studies<sup>1,2</sup> in the use of microscopic models, which are capable of predicting the absolute value of the shift rather than only the relative trend upon changing the solvent polarity.

We have incorporated the effect of the solvent induced dipoles both in the simplified LD model and in the all-atom MD study. The inclusion of the induced dipoles appears to be much more important for evaluation of excited-state properties than for ground-state properties. That is, in the ground state, the permanent dipoles orient themselves toward the solute charges and the field from the induced dipoles is rather small. In the excited state, on the other hand, the permanent dipoles may not be oriented toward the solute charges and the effect of the induced dipoles is much more important. Thus, it seems that calculations that neglect the effect of the solvent induced dipoles are unlikely to provide reliable results (regardless of the quantum mechanical method used for the evaluation of excitation energies and the solute charge distribution).

This work did not explore the change in solvent effects between different polar solvents (e.g., between water and ethanol). Such changes are clearly observed experimentally, and some of them can be attributed to local hydrogen bonding.<sup>3d</sup> These effects may be accounted for by the LD model but would require not only change of the effective dipole moment,  $m_0$ , between different solvents but also (and maybe more importantly) changes of the solute-solvent radius  $R_w$ . Obviously, specific solvent effects are expected to be represented reliably by the SCAAS model, but actual studies that address this issue are clearly needed.

The present study leaves several problems open. In particular, we did not address the spectral shift associated with moving molecules from gas phase to nonpolar solvents, when the solute charge distribution does not change significantly upon excitation. This interesting effect might be due to the fact that the solute electrons experience different effective potentials in the gas phase and in solution, even when the solvent is not polarized by the solute. For example, if we consider a hydrogen atom surrounded by a simple "solvent" shell of four He atoms, we will find that the 1s hydrogen electron is more stable near a He atom than at the corresponding point in vacuum. This means that the effective atomic orbitals of the solute will be less localized around their nuclear cores. Such an effect may be represented by considering the attraction between the solute electrons and the solvent atoms, representing the solvent effect by a pseudopotential (note that we are referring here to an effect that is not related to the solvent polarization and is not treated by eq 5). However, it is reasonable to assume that the above solvent shift is similar in polar and nonpolar solvents. It is also quite likely that this effect is taken into account by the fact that our semiempirical integrals are parametrized by using solution spectra. Nevertheless, it is clear that this shift requires more serious attention. Another open question is associated with the change in line shape upon moving the solute from polar to nonpolar solvents. This challenging problem can be analyzed with the dispersed polaron model presented here, but such a task will be delayed to a subsequent study.

Finally it may be useful to comment about the potential of our approach in analyzing the spectra of biological chromophores. Such studies have been used traditionally as a way to examine different structural hypotheses. Now, when many protein structures are known, the challenge is inverted. One would like



to use the known structure of the protein–chromophore complex and to reproduce the observed spectral shifts of the chromophore. In this way, one can use the agreement between the calculated and observed environmental effects to validate calculations of electrostatic potentials in proteins.<sup>4b</sup> The present approach may provide a powerful general way for structure–spectra correlations in proteins. Such studies can be performed by either the Protein Dipole Langevin Dipole<sup>46</sup> method (which substitutes the LD model in protein environments) or with the protein version of the SCAAS method.<sup>26</sup> Both approaches can now be conveniently used for studies of the spectra of biological chromophores with the program package MOLARIS.<sup>16</sup>

**Acknowledgment.** This work was supported by the National Institute of Health, Grant GM-24492, and the office of Naval Research, Contract No. N00014-87-K-0507.

## Appendix

Our induced dipole treatment that might look like an ad hoc approach can be derived starting with traditional perturbation treatments of solvent effects on absorption spectra.<sup>1,2</sup> This will be done below deriving both the standard diagonal correction that leads to eq 15 and a new off-diagonal interaction term.

We start here following the approach of ref 2c and expressing the solute–solvent system as

$$H = H_S + H_s + H_{Ss}' \quad (30)$$

where  $H_{Ss}'$  is the solute–solvent interaction term, which is treated as a perturbation. Expanding  $H_{Ss}'$ , one obtains

$$H_{Ss}' \approx \sum_t R_{St}^{-3} \mathbf{M}^S \theta_{St} \mathbf{M}^t \quad t \in s \quad (31)$$

where  $t$  runs over the solvent molecules and  $\mathbf{M}^t$ 's are the dipole operators given by

$$\mathbf{M}^S = \sum_A z_A \mathbf{R}_A - \sum_\alpha r_\alpha \quad (32)$$

where  $z_A$  and  $\mathbf{R}_A$  are the charge and position of the  $A$ th nucleus and  $r_\alpha$  is the position of the  $\alpha$ th electron. A similar expression is used for  $\mathbf{M}^t$ . The tensor  $\theta$  in eq 31 is defined by

$$\theta = \mathbf{I} - 3\hat{\mathbf{e}}\hat{\mathbf{e}} \quad (33)$$

Here  $\mathbf{I}$  is the unit matrix and  $\hat{\mathbf{e}}$  is the unit vector in the direction of  $\mathbf{R}_{st}$  so that  $(\hat{\mathbf{e}}\hat{\mathbf{e}})_{\alpha\beta} = R_{st}^\alpha R_{st}^\beta / R_{st}^2$ , where  $R^\alpha$  is the  $\alpha$ th Cartesian component of  $\mathbf{R}$ .

Now we can approximate our system by the wave functions

$$\Psi_{f0} = \Psi_S^f \phi_1^0 \phi_2^0 \dots \phi_i^0 \dots \phi_N^0 \quad (34)$$

$$\Psi_{fn} = \Psi_S^f \phi_1^0 \phi_2^0 \dots \phi_i^n \dots \phi_N^0$$

where the  $\phi$ 's designate here the state functions of the solvent molecules, and we only consider wave functions with at most one solvent molecule in its virtual excited state. Using first-order perturbation theory (which considers only the basis set of eq 34 and neglects simultaneous excitations of several solvent molecules), we obtain<sup>2c</sup>

$$\begin{aligned} \Delta E^{(1)} &= \langle \Psi_{f0} | H' | \Psi_{f0} \rangle \\ &= \sum_{i=1}^N R_{Si}^{-3} \langle \Psi_S^f \phi_i^0 | \mathbf{M}^S \theta_{Si} \mathbf{M}^i | \Psi_S^f \phi_i^0 \rangle \\ &= \sum_{i=1}^N \mu_S^f \theta_{Si} \mu_i^0 \approx \sum_A \sum_t \sum_{B(t)} Q_A^f q_{E(t)}^0 / R_{AB(t)} = V_f^{\text{perm}} \end{aligned} \quad (35)$$

where  $\mu_i^0 = \langle \phi_i^0 | \mathbf{M}^i | \phi_i^0 \rangle$  and  $\mu_S^f = \langle \Psi_S^0 | \mathbf{M}^S | \Psi_S^f \rangle$  and  $B(t)$  indicates that the atom  $B$  is attached to the  $t$ th solvent molecule. In deriving the last terms of eq 35, we replace the dipole–dipole interaction term by the corresponding monopole–monopole interaction.

Next we can proceed to second-order perturbation treatment, which gives<sup>2c</sup>

$$\begin{aligned} \Delta E_S^{(2)} &= -\frac{1}{2} \sum_t R_{St}^{-6} \mu_S^f \theta_{St} \alpha_t \theta_{St} \mu_S^f \approx -\frac{1}{2} \sum_t \xi_t^f \alpha_t \xi_t^f \approx \\ &\quad \frac{1}{2} \sum_A Q_A^f U_{Af}^{\text{ind}} = V_{\text{ind}}^f \end{aligned} \quad (36)$$

where

$$\alpha_t = 2 \sum_n \frac{\langle \phi_i^0 | \mathbf{M}^i | \phi_i^n \rangle \langle \phi_i^n | \mathbf{M}^i | \phi_i^0 \rangle}{\epsilon_t^n - \epsilon_t^0} \quad (37)$$

Here we replace the interactions between the field of the solute  $\xi_t^f$  and the solvent induced dipoles ( $\mu_t = \alpha_t \xi_t^f$ ) by the equivalent interaction between the potential from the solvent induced dipoles and the solute charges.

Similarly we find for the interaction between the solute induced dipoles and the potential from the solvent

$$\Delta E_S^{(2)} = -\frac{1}{2} \xi_S \alpha_S^f \xi_S \approx \Delta E_f^S \quad (38)$$

where this type of term leads in the classical model to the  $\Delta \Delta E_{gf}^S$  of eq 12. Note, however, that the second-order perturbation treatment *does not* include the self-consistent interaction between the induced dipoles themselves). The classical estimate of  $\Delta E_f^S$  can also be obtained by writing

$$\Delta E_f^S = \frac{1}{2} \sum_A [Q_{Af}(U_f) - Q_{Af}(0)] U_{Af} = \frac{1}{2} \sum_A \Delta Q_{Af} U_{Af} \quad (39)$$

where we exploit the fact that half of the energy gained from the interaction between an induced dipole and the corresponding external potential is invested in polarizing the dipole (or in changing the charges from their unperturbed value).

Note that, in the derivation of eqs 30–39, we did not make any statement about the specific solvent model, and this is not much different than the treatment in section 2 (except the explicit quantum mechanical evaluation of  $\Delta \Delta E_{gf}^S$ ). Thus, the main problem with the classical derivation is not the perturbation treatment but the continuum solvent model with the arbitrarily selected cavity radius.

Finally, it is interesting to note that the second-order perturbation treatment that leads to eq 36 gives an off-diagonal mixing term between different solute states by

$$\langle \Psi_S^f | H' | \Psi_S^{f'} \rangle = -\frac{1}{2} \sum_t R_{St}^{-6} \mu_S^{ff'} \theta_{St} \alpha_t \theta_{St} \mu_S^{ff'} \quad (40)$$

where  $\mu_S^{ff'}$  is the transition dipole  $\langle \Psi_S^f | \mathbf{M}^S | \Psi_S^{f'} \rangle$ . This term can be implemented with the same type of induced dipole treatment introduced in eq 36 (considering now the solute transition charges,  $Q_A^{ff'}$ , rather than the excited-state charges,  $Q_A^f$ ) and used in a treatment that considers solvent-induced mixing between the solute states.

(26) Warshel, A.; Sussman, F.; King, G. *Biochemistry* 1986, 25, 8368.